

Drell-Yan lepton pair production at LHC and TMD quark densities of the proton

S.P. Baranov¹, A.V. Lipatov^{2,3}, N.P. Zotov²

March 4, 2014

¹*P.N. Lebedev Institute of Physics, 119991 Moscow, Russia*

²*Skobeltsyn Institute of Nuclear Physics, Lomonosov Moscow State University, 119991 Moscow, Russia*

³*Joint Institute for Nuclear Research, 141980 Dubna, Moscow Region, Russia*

Abstract

We use the TMD quark densities of the proton to investigate unpolarized Drell-Yan lepton pair production in proton-proton collisions at the LHC energies. We investigate the case where the gluon-to-quark splitting occurs at the last evolution step and calculate the TMD sea quark density as a convolution of the CCFM-evolved gluon distribution and the TMD gluon-to-quark splitting function which contains all single logarithmic small- x corrections to the sea quark evolution for any order of perturbation theory. Based on the $\mathcal{O}(\alpha)$ production amplitude $q^* + \bar{q}^* \rightarrow Z/\gamma^* \rightarrow l^+ + l^-$ which calculated according to the reggeized quark approach, we analyze the distributions on the dilepton invariant mass, transverse momentum and rapidity as well as the specific angular correlations between the produced leptons as measured by the CMS, ATLAS and LHCb collaborations. We argue that these measurements impose stringent constraints on the TMD quark distributions of the proton.

PACS number(s): 12.38.-t, 12.15.Ji

1 Introduction

Usually, the scale-dependent quark and gluon densities are calculated as a function of Bjorken variable x and hard scale μ^2 within the framework of the DGLAP evolution equations [1] based on the standard collinear QCD factorization. However, for a wide class of semi-inclusive processes probing the small- x and forward physics at the LHC it is more appropriate to use the parton distributions unintegrated over the partonic transverse momentum k_T or, transverse momentum dependent (TMD) parton distributions [2]. The latter are subject of intense studies, and various approaches to investigate these quantities have been proposed [3–6]. At asymptotically large energies (or very small x) the theoretically correct description is based on the BFKL evolution equation [7] where the leading $\ln(1/x)$ contributions are taken into account to all orders. Another approach, which is valid for both small and large x , is given by the CCFM gluon evolution equation [8]. In the limit of asymptotic high energies, it is equivalent to BFKL, but also similar to the DGLAP evolution for large x . Two basic TMD gluon densities are used in the small- x formalism: the so-called Weizsaker-Williams and the dipole ones [9–11].

Most of previous phenomenological applications of the TMD parton distributions in the framework of high energy QCD factorization (or k_T -factorization approach) [12, 13] take only gluon and valence quark contributions into account (see, for example, [14–18]). Such approaches are reasonable approximations, based on the dominance of spin-1 exchange processes at high energies, for the production processes coupled to the gluons (such as, for example, production of heavy flavours or scalar particles). However, to correctly treat the final states associated with the quark-initiated processes it is necessary to go beyond this simple approximation and take into account subleading effects. First attempts to address this issue and evaluate the TMD sea quark density have been performed in [19–22], where the relevant TMD gluon distribution has been derived via splitting probabilities to lowest order of perturbative theory, neglecting any transverse momentum dependence in the gluon-to-quark branching. In [23] the TMD kinematic corrections have been included, while the splitting kernels are still taken at lowest order. Recently, the TMD sea quark densities have been calculated [24] incorporating the effects of the TMD gluon-to-quark splitting function [25] which contains all single logarithmic small- x corrections to sea quark evolution for any order of perturbation theory, and the kinematical effects from initial state parton transverse momentum on the forward Z boson spectrum have been studied. The proposed formulation [24–26] has been implemented in a Monte Carlo event generator CASCADE [27]. In the present paper we apply the TMD sea quark densities [24] to investigate the Drell-Yan lepton pair production at the LHC. This process, where quark-antiquark annihilation form a intermediate virtual photon γ^* or Z boson decaying to lepton pairs, offers high sensitivity to the sea quark evolution of a proton.

The production of Drell-Yan lepton pairs at the LHC is subject of intense studies from both theoretical and experimental points of view [28–35]. It provides a major source of background to a number of processes, such as Higgs, $t\bar{t}$ -pair, di-boson or W' and Z' bosons production and other processes beyond the Standard Model. It is an important reference process for measurements of electroweak boson properties, and it is used for monitoring of the collider luminosity and calibration of detectors. A first study of Drell-Yan process at the TMD level has been performed in [36], where diagrams with virtual photon exchange only are considered and mostly on the rather low energies covered by the RHIC and UA1 experiments are covered. A more recent investigation [37] was based on the $\mathcal{O}(\alpha)$ and $\mathcal{O}(\alpha\alpha_s)$ production amplitudes of $q + \bar{q} \rightarrow Z/\gamma^* \rightarrow l^+ + l^-$ and $q + g^* \rightarrow Z/\gamma^* + q \rightarrow l^+ + l^- + q$ subprocesses where only the initial gluon transverse momentum has been taken

into account. This process has been investigated also in the framework of the soft-collinear effective theory [38, 39], and general investigation of high energy resummation for Drell-Yan lepton pair production has been done in [40]. In the present paper we concentrate on the off-shell (or transverse momentum dependent) quark-antiquark annihilation $q^* + \bar{q}^* \rightarrow Z/\gamma^* \rightarrow l^+ + l^-$ and calculate the corresponding production amplitude according to the reggeized quark approach [41, 42], which is based on the effective action formalism [43], currently explored at next-to-leading order [44]. It was shown that the use of effective vertices [41, 42] ensures the exact gauge invariance of calculated amplitude despite the off-shell initial quarks. We apply the TMD valence and sea quark distributions [15, 24] to calculate the Drell-Yan production cross sections at LHC energies. For comparison, we also use the TMD quark densities obtained in the Kimber-Martin-Ryskin (KMR) scheme [20, 21]. We analyze the dilepton transverse momentum and rapidity distributions as well as the specific angular correlations between the produced leptons and compare our predictions with recent data taken by the CMS [28–30], ATLAS [31–34] and LHCb [35] collaborations. Note that we present a first phenomenological application of the formalism developed in [24, 25] to the analysis of experimental data.

The outline of our paper is following. In Section 2 we recall shortly the basic formulas of k_T -factorization QCD approach. The TMD quark densities are discussed in Section 3. In Section 4 we present numerical results of our calculations. Section 4 contains our conclusions.

2 Theoretical framework

Our consideration is based on the $\mathcal{O}(\alpha)$ subprocess of off-shell quark-antiquark annihilation into a virtual photon or Z boson which decays to lepton pair:

$$q^*(q_1) + \bar{q}^*(q_2) \rightarrow Z/\gamma^* \rightarrow l^+(p_1) + l^-(p_2), \quad (1)$$

where the four-momenta of all corresponding particles are given in the parentheses. Note that $\mathcal{O}(\alpha\alpha_s)$ contributions from $q^* + g^* \rightarrow Z/\gamma^* + q \rightarrow l^+ + l^- + q$ and $q^* + \bar{q}^* \rightarrow Z/\gamma^* + g \rightarrow l^+ + l^- + g$ subprocesses are effectively taken into account in our consideration due to the initial state gluon radiation. This is in contrast with collinear QCD factorization where all these contributions have to be taken into account separately¹.

Within the reggeized quark formalism [41, 42], the off-shell amplitude of $q^* + \bar{q}^* \rightarrow Z/\gamma^* \rightarrow l^+ + l^-$ subprocess can be written as

$$\mathcal{M}_\gamma = e_q e^2 \bar{v}_{s_1}(q_2) \Gamma_\gamma^\mu(q_1, q_2) u_{s_2}(q_1) \frac{g^{\mu\nu}}{\hat{s}} \bar{u}_{r_1}(p_1) \gamma^\nu v_{r_2}(p_2), \quad (2)$$

$$\begin{aligned} \mathcal{M}_Z = & \frac{e^2}{\sin 2\theta_W} \bar{v}_{s_1}(q_2) \Gamma_Z^\mu(q_1, q_2) u_{s_2}(q_1) \left[g^{\mu\nu} - \frac{(q_1 + q_2)^\mu (q_1 + q_2)^\nu}{m_Z^2} \right] \times \\ & \times \frac{1}{\hat{s} - m_Z^2 - im_Z \Gamma_Z} \bar{u}_{r_1}(p_1) \gamma^\nu (C_V^l - C_A^l \gamma^5) v_{r_2}(p_2), \end{aligned} \quad (3)$$

where e and e_q are the electron and quark (fractional) electric charges, $\hat{s} = (q_1 + q_2)^2$, m_Z and Γ_Z are the mass and full decay width of Z boson, θ_W is the Weinberg mixing angle, C_V^l and C_A^l are the vector and axial lepton coupling constants, and the transverse momenta of initial quarks are $\mathbf{q}_{1T}^2 \neq 0$ and $\mathbf{q}_{2T}^2 \neq 0$. We take the propagator of the intermediate Z boson in the Breit-Wigner form to avoid any artificial singularities in

¹See, for example, reviews [2] for more information.

the numerical calculations. The effective vertex $\Gamma_\gamma^\mu(q_1, q_2)$ which describes the effective coupling of off-shell (reggeized) quark and antiquark to the photon reads [41, 42]

$$\Gamma_\gamma^\mu(q_1, q_2) = \gamma^\mu - \hat{q}_1 \frac{l_1^\mu}{q_2 \cdot l_1} - \hat{q}_2 \frac{l_2^\mu}{q_1 \cdot l_2}, \quad (4)$$

where l_1 and l_2 are the four-momenta of colliding protons. The coupling of the off-shell quark and antiquark to the Z boson is constructed in a similar way:

$$\Gamma_Z^\mu(q_1, q_2) = \Gamma_\gamma^\mu(q_1, q_2)(C_V^q - C_A^q \gamma^5), \quad (5)$$

where C_V^q and C_A^q are the corresponding vector and axial coupling constants. The effective vertexes $\Gamma_\gamma^\mu(q_1, q_2)$ and $\Gamma_Z^\mu(q_1, q_2)$ satisfy the Ward identities $\Gamma_\gamma^\mu(q_1, q_2)(q_1 + q_2)_\mu = 0$ and $\Gamma_Z^\mu(q_1, q_2)(q_1 + q_2)_\mu = 0$. It is obvious that the amplitudes (4) and (5) are gauge invariant despite the off-shell initial quarks. In all other respects the evaluation follows the standard QCD Feynman rules. The further calculation (including $\gamma^* - Z$ interference) is straightforward and was done using the algebraic manipulation system FORM [45]. We do not list here explicitly the lengthy expressions. In the on-shell limit, with $\mathbf{q}_{1T}^2 \rightarrow 0$ and $\mathbf{q}_{2T}^2 \rightarrow 0$, we recover the well-known textbook formulas.

To calculate the total and differential cross sections one has to convolute the evaluated off-shell amplitude squared $|\bar{\mathcal{M}}|^2$ with the TMD quark densities of the proton. Our master formula reads:

$$\sigma = \sum_q \int \frac{|\bar{\mathcal{M}}|^2}{16\pi (x_1 x_2 s)^2} f_q(x_1, \mathbf{q}_{1T}^2, \mu^2) f_q(x_2, \mathbf{q}_{2T}^2, \mu^2) d\mathbf{p}_{1T}^2 d\mathbf{q}_{1T}^2 d\mathbf{q}_{2T}^2 dy_1 dy_2 \frac{d\phi_1}{2\pi} \frac{d\phi_2}{2\pi}, \quad (6)$$

where s is the total energy, y_1 and y_2 are the center-of-mass rapidities of the produced leptons, ϕ_1 and ϕ_2 are the azimuthal angles of the initial quarks having the fractions x_1 and x_2 of the longitudinal momenta of the colliding protons. Finally, from the conservation laws one can easily obtain the following relations:

$$\mathbf{q}_{1T} + \mathbf{q}_{2T} = \mathbf{p}_{1T} + \mathbf{p}_{2T}, \quad (7)$$

$$x_1 \sqrt{s} = m_{1T} e^{y_1} + m_{2T} e^{y_2}, \quad (8)$$

$$x_2 \sqrt{s} = m_{1T} e^{-y_1} + m_{2T} e^{-y_2}, \quad (9)$$

where \mathbf{p}_{1T} and \mathbf{p}_{2T} are the transverse momenta of produced leptons, and m_{1T} and m_{2T} are their transverse masses.

3 TMD quark densities

In the present paper we concentrate on the CCFM approach to calculate the TMD parton densities of the proton. As it was already mentioned above, the CCFM parton shower, based on the principle of color coherence, describes only the emission of gluons, while real quark emissions are left aside. It implies that the CCFM equation describes only the distinct evolution of TMD gluon and valence quarks, while the non-diagonal transitions between quarks and gluons are absent. The TMD gluon [46] and valence quark [15] distributions $f_g(x, \mathbf{k}_T^2, \mu^2)$ and $f_q^{(v)}(x, \mathbf{q}_T^2, \mu^2)$ have been obtained from the numerical solutions of the CCFM equation. Here \mathbf{k}_T and \mathbf{q}_T are the gluon and quark transverse momenta, respectively. In the approximation where the sea quarks occur in the last

gluon-to-quark splitting, the TMD sea quark density at the next-to-leading logarithmic accuracy $\alpha_s(\alpha_s \ln x)^n$ can be written [24] as follows:

$$f_q^{(s)}(x, \mathbf{q}_T^2, \mu^2) = \int_x^1 \frac{dz}{z} \int d\mathbf{k}_T^2 \frac{1}{\Delta^2} \frac{\alpha_s}{2\pi} P_{qg}(z, \mathbf{k}_T^2, \Delta^2) f_g(x/z, \mathbf{k}_T^2, \bar{\mu}^2), \quad (10)$$

where z is the fraction of the gluon light cone momentum which is carried out by the quark, and $\Delta = \mathbf{q}_T - z\mathbf{k}_T$. The sea quark evolution is driven by the off-shell gluon-to-quark splitting function $P_{qg}(z, \mathbf{k}_T^2, \Delta^2)$ [25]:

$$P_{qg}(z, \mathbf{k}_T^2, \Delta^2) = T_R \left(\frac{\Delta^2}{\Delta^2 + z(1-z)\mathbf{k}_T^2} \right)^2 \left[(1-z)^2 + z^2 + 4z^2(1-z)^2 \frac{\mathbf{k}_T^2}{\Delta^2} \right], \quad (11)$$

with $T_R = 1/2$. The splitting function $P_{qg}(z, \mathbf{k}_T^2, \Delta^2)$ has been obtained by generalizing to finite transverse momenta, in the high-energy region, the two-particle irreducible kernel expansion [47]. Although evaluated off-shell, this splitting function is universal [25]. It takes into account the small- x enhanced transverse momentum dependence up to all orders in the strong coupling, and reduces to the collinear splitting function at lowest order for $\mathbf{k}_T^2 \rightarrow 0$. The scale $\bar{\mu}^2$ is defined [24] from the angular ordering condition which is natural from the point of view of the CCFM evolution: $\bar{\mu}^2 = \Delta^2/(1-z)^2 + \mathbf{k}_T^2/(1-z)$. To precise, in (10) we have used A0 gluon [46].

Beside the CCFM-based approximation above, to determine the TMD quark densities in a proton we have used also the Kimber-Martin-Ryskin (KMR) approach [20, 21]. This approach is a formalism to construct the TMD parton distributions from the known collinear ones. In this approximation, the TMD quark densities are given by [20, 21]

$$f_q(x, \mathbf{q}_T^2, \mu^2) = T_q(\mathbf{q}_T^2, \mu^2) \frac{\alpha_s(\mathbf{q}_T^2)}{2\pi} \times \times \int_x^1 dz \left[P_{qq}(z) \frac{x}{z} q\left(\frac{x}{z}, \mathbf{q}_T^2\right) \Theta(\varsigma - z) + P_{qg}(z) \frac{x}{z} g\left(\frac{x}{z}, \mathbf{q}_T^2\right) \right], \quad (12)$$

where $P_{ab}(z)$ are the unregulated leading-order DGLAP splitting functions. The theta function in (12) implies the angular-ordering constraint $\varsigma = \mu/(\mu + |\mathbf{q}_T|)$ specifically to the last evolution step to regulate the soft gluon singularities. The Sudakov form factor $T_q(\mathbf{q}_T^2, \mu^2)$ enable us to include logarithmic loop corrections to the calculated cross sections. In the region of small $\mathbf{q}_T^2 < \mu_0^2$, where $\mu_0^2 \sim 1 \text{ GeV}^2$ is the minimum scale for which the DGLAP evolution of the initial parton densities is valid, the TMD quark distributions are defined from the normalisation condition:

$$f_q(x, \mathbf{q}_T^2, \mu^2)|_{\mathbf{q}_T^2 < \mu_0^2} = xq(x, \mu_0^2)T_q(\mu_0^2, \mu^2). \quad (13)$$

For the numerical calculations we have used the leading-order MSTW'2008 parton densities [48].

The calculated TMD up, down and light sea quark densities are shown in Fig. 1 as a function of \mathbf{q}_T^2 for different values of x at $\mu^2 = m_Z^2$. Even with very different approaches, the TMD quark densities are rather similar at large \mathbf{q}_T^2 . The influence of starting distributions and/or initial conditions is concentrated at small values of \mathbf{q}_T^2 . It was pointed out [18] that the small \mathbf{q}_T^2 region provides information on the non-perturbative part of the TMD parton density functions. The difference between the CCFM-based and KMR approaches are visible clearly in the sea quark distributions which are driven mainly by the gluon densities.

4 Numerical results

We now are in a position to present our numerical results. After we fixed the TMD quark densities, the cross section (6) depends on the renormalization and factorization scales μ_R and μ_F . Numerically, we set them to be equal to $\mu_R = \mu_F = \xi M$, where M is the invariant mass of produced lepton pair. To estimate the scale uncertainties of our calculations we vary the parameter ξ between $1/2$ and 2 about the default value $\xi = 1$. Following to [49], we set $m_Z = 91.1876$ GeV, $\Gamma_Z = 2.4952$ GeV, $\sin^2 \theta_W = 0.23122$ and use the LO formula for the strong coupling constant $\alpha_s(\mu^2)$ with $n_f = 4$ active quark flavors at $\Lambda_{\text{QCD}} = 200$ MeV, so that $\alpha_s(m_Z^2) = 0.1232$. Since we investigate a wide region of M , we use the running QED coupling constant $\alpha(\mu^2)$. To take into account the non-logarithmic loop corrections to the quark-antiquark annihilation cross section we apply the effective K -factor, as it was done in [21, 37]:

$$K = \exp \left[C_F \frac{\alpha_s(\mu^2)}{2\pi} \pi^2 \right], \quad (14)$$

where color factor $C_F = 4/3$. A particular scale choice $\mu^2 = \mathbf{p}_T^{4/3} M^{2/3}$ (with \mathbf{p}_T being the transverse momentum of produced lepton pair) has been proposed [21, 50] to eliminate sub-leading logarithmic terms. We choose this scale to evaluate the strong coupling constant in (14) only. Everywhere the multidimensional integration have been performed by the means of Monte Carlo technique, using the routine VEGAS [51]. The corresponding C++ code is available from the authors on request².

Experimental data for the Drell-Yan production at the LHC come from the CMS [28–30], ATLAS [31–34] and LHCb [35] collaborations. The CMS collaboration has reported the normalized dilepton invariant mass distribution measured at $15 < M < 600$ GeV [28]. The normalized dilepton rapidity y and transverse momentum distributions have been measured in the Z boson mass region $60 < M < 120$ GeV [29]. The ATLAS and LHCb collaborations have presented the differential cross sections in the central ($|y| < 3.5$) and forward ($2 < y < 4.5$) dilepton rapidity regions at $66 < M < 116$ GeV [31–33, 35]. Very recently the ATLAS collaboration has measured the Drell-Yan differential cross-section as a function of dilepton invariant mass in the range $116 < M < 1500$ GeV [34]. Note that special cuts on the pseudorapidities and transverse momenta of produced leptons have been applied in all these measurements, see [28–35] for the detailed information. Of course, we impose these cuts in the same manner as it was done in the experimental analyses.

The results of our calculations are presented in Figs. 2 — 6 in comparison with the LHC data. The differential cross sections as a function of dilepton invariant mass and rapidity are shown in Figs. 2 and 3. We find that these distributions are described reasonably well by the CCFM-based calculations. However, the KMR predictions significantly (by a factor of about 2) underestimate the LHC data, mainly due to different behaviour of corresponding TMD sea quark densities at low transverse momenta (see Fig. 1). We observe that the shape of dilepton invariant mass distributions is not very sensitive to the TMD quark densities. This is in a contrast with the distributions on the dilepton rapidity, where the CCFM and KMR predictions differ from each other (Fig. 3). The sensitivity of predicted cross sections to the TMD quark densities is also clearly visible in the transverse momentum distributions of produced lepton pair, or in the distributions of the ϕ_η^* variable, as it is shown in Figs. 4 and 5. The ϕ_η^* variable is defined as [52–54]:

$$\phi_\eta^* = \tan \left(\frac{\phi_{\text{acop}}}{2} \right) \left[\cosh \left(\frac{\Delta\eta}{2} \right) \right]^{-1}, \quad (15)$$

²lipatov@theory.sinp.msu.ru

where $\phi_{\text{acop}} = \pi - |\Delta\phi|$ is the acoplanarity angle, and $\Delta\eta$ and $\Delta\phi$ are the differences in pseudorapidity and azimuthal angles between the leptons, respectively. The variable ϕ_η^* is correlated to the quantity $|\mathbf{p}_T|/M$ and therefore probes the same physics as the dilepton transverse momentum [55–57]. Note that both these observables are singular at leading order in the collinear QCD approximation due to back-to-back kinematic, whereas in the k_T -factorization approach the finite transverse momentum of lepton pair is generated already in simple quark-antiquark annihilation (1). One can see that none of the TMD quark densities under consideration describe well the transverse momentum and ϕ_η^* distributions, although their shapes are better reproduced by the KMR predictions. The CCFM-based calculations overestimate the CMS [29] and ATLAS [32] data (taken in a central dilepton rapidity region) at low transverse momenta and underestimate them if dilepton transverse momentum increases. We note, however, that description of these observables is improved if higher order contributions (which, in particular, affect on the shape of transverse momentum distributions) are taken into account [37]. In a forward dilepton rapidity region, the CCFM predictions agree well with the LHCb data (see Fig. 5).

According to (2) and (3), the off-shell amplitude of the Drell-Yan production subprocess contains both the vector and axial-vector couplings of Z boson to fermions. The corresponding differential cross section (6) can be described by the polar and azimuthal angles of produced leptons in their rest frame. When integrated over the azimuthal angle, it can be presented as follows:

$$\frac{d\sigma}{d\cos\theta^*} \sim \frac{3}{8}(1 + \cos^2\theta^*) + A_{\text{FB}} \cos\theta^*, \quad (16)$$

where θ^* is the emission angle of produced lepton with respect to the quark momentum in the dilepton rest frame, and A_{FB} is the parameter of forward-backward asymmetry. It is defined as

$$A_{\text{FB}} = \frac{\sigma_{\text{F}} - \sigma_{\text{B}}}{\sigma_{\text{F}} + \sigma_{\text{B}}}, \quad (17)$$

where σ_{F} and σ_{B} are the total cross sections for forward and backward events, i.e. events with positive or negative values of $\cos\theta^*$. At the dilepton invariant masses near the Z boson peak, the asymmetry A_{FB} is predicted to be small due to the small value of the lepton vector coupling. Above and below the Z boson peak, A_{FB} shows a characteristic energy dependence governed by $\gamma^* - Z$ interference. Deviations from the Standard Model predictions for A_{FB} may indicate the existence of new particles beyond the Standard Model. Recently the CMS collaboration has presented [30] a first measurement of the asymmetry A_{FB} . Our predictions for A_{FB} as a function of the dilepton invariant mass and rapidity are shown in Fig. 6 in comparison with the CMS data. Following to experimental procedure [30], we use the Collins-Soper frame where θ^* is defined to be the angle between the lepton momentum and the axis that bisects the angle between the direction of one proton and the direction opposite to the other proton. We find a good agreement of our predictions and the CMS data as was also obtained with collinear QCD calculations [30]. In contrast with the dilepton transverse momentum and rapidity distributions, there is practically no differences between the CCFM-based and KMR predictions for A_{FB} . Note that the angular distributions in dilepton production at the Tevatron have been investigated in [37].

To conclude, we have demonstrated that the studies of Drell-Yan production (in particular, investigations of the dilepton transverse momentum and rapidity distributions) impose a stringent constraints on the TMD quark densities in a proton. Moreover, this process can be used as an important tool to determine the parameters of initial (starting)

TMD parton distributions. It is important for further investigations of small- x physics at hadron colliders, in particular, in the direction which concerns the non-linear effects originating from high parton densities at small x .

5 Conclusion

We used the TMD quark densities in a proton to investigate unpolarized Drell-Yan lepton pair production in pp collisions at the LHC energies. We investigated the case where the gluon-to-quark splitting occurs at the last evolution step and calculated the TMD sea quark density as a convolution of the CCFM-evolved gluon distribution and TMD gluon-to-quark splitting function. This function contains all single logarithmic small- x corrections to sea quark evolution for any order of perturbation theory. We calculated $\mathcal{O}(\alpha)$ production amplitude $q^* + \bar{q}^* \rightarrow Z/\gamma^* \rightarrow l^+ + l^-$ within the reggeized (off-shell) quark approach which ensures the exact gauge invariance. The higher-order $\mathcal{O}(\alpha\alpha_s)$ subprocesses $q^* + g^* \rightarrow Z/\gamma^* + q \rightarrow l^+ + l^- + q$ and $q^* + \bar{q}^* \rightarrow Z/\gamma^* + g \rightarrow l^+ + l^- + g$ are present in calculations as part of the evolution of TMD parton densities. We have analyzed the distributions on the dilepton invariant mass, transverse momentum and rapidity as well as the specific angular correlations between the produced leptons as measured by the CMS, ATLAS and LHCb collaborations. These measurements impose a stringent constraints on the TMD quark distributions in a proton. We obtain a reasonably good description of the experimental measurements with our approach.

Acknowledgements

We thank H. Jung for careful reading the manuscript and very useful remarks. The authors are also grateful to F. Hautmann and S. Marzani for discussions and comments. This research was supported by the FASI of Russian Federation (grant NS-3042.2014.2), RFBR grant 13-02-01060 and the grant of the Ministry of education and sciences of Russia (agreement 8412). The authors are also grateful to DESY Directorate for the support in the framework of Moscow—DESY project on Monte-Carlo implementation for HERA—LHC.

References

- [1] V.N. Gribov and L.N. Lipatov, Sov.J. Nucl. Phys. **15**, 438 (1972);
L.N. Lipatov, Sov. J. Nucl. Phys. **20**, 94 (1975);
G. Altarelli, G. Parisi, Nucl. Phys. B **126**, 298 (1977);
Yu.L. Dokshitzer, Sov. Phys. JETP **46**, 641 (1977).
- [2] B. Andersson *et al.* (Small- x Collaboration), Eur. Phys. J. C **25**, 77 (2002);
J. Andersen *et al.* (Small- x Collaboration), Eur. Phys. J. C **35**, 67 (2004);
J. Andersen *et al.* (Small- x Collaboration), Eur. Phys. J. C **48**, 53 (2006).
- [3] J.C. Collins, *Foundations of perturbative QCD*, Cambridge University Press, 2011.
- [4] E. Avsar, arXiv:1108.1181 [hep-ph]; arXiv:1203.1916 [hep-ph].
- [5] F. Dominguez, C. Marquet, B.-W. Xiao, F. Yuan, Phys. Rev. D **83**, 105005 (2011).
- [6] S.M. Aybat, T.C. Rogers, Phys. Rev. D **83**, 114042 (2011).

- [7] E.A. Kuraev, L.N. Lipatov, V.S. Fadin, Sov. Phys. JETP **44**, 443 (1976);
E.A. Kuraev, L.N. Lipatov, V.S. Fadin, Sov. Phys. JETP **45**, 199 (1977);
I.I. Balitsky, L.N. Lipatov, Sov. J. Nucl. Phys. **28**, 822 (1978).
- [8] M. Ciafaloni, Nucl. Phys. B **296**, 49 (1988);
S. Catani, F. Fiorani, G. Marchesini, Phys. Lett. B **234**, 339 (1990);
S. Catani, F. Fiorani, G. Marchesini, Nucl. Phys. B **336**, 18 (1990);
G. Marchesini, Nucl. Phys. B **445**, 49 (1995).
- [9] J.-W. Qiu, P. Sun, B.-W. Xiao, F. Yuan, arXiv:1310.2230 [hep-ph].
- [10] P. Sun, C.-P. Yuan, F. Yuan, Phys. Rev. D **88**, 054008 (2013).
- [11] A.H. Mueller, B.-W. Xiao, F. Yuan, arXiv:1308.2993 [hep-ph].
- [12] L.V. Gribov, E.M. Levin, M.G. Ryskin, Phys. Rep. **100**, 1 (1983);
E.M. Levin, M.G. Ryskin, Yu.M. Shabelsky, A.G. Shuvaev, Sov. J. Nucl. Phys. **53**, 657 (1991).
- [13] S. Catani, M. Ciafaloni, F. Hautmann, Nucl. Phys. B **366**, 135 (1991);
J.C. Collins, R.K. Ellis, Nucl. Phys. B **360**, 3 (1991).
- [14] F. Hautmann, H. Jung, JHEP **0810**, 113 (2008).
- [15] M. Deak, H. Jung, K. Kutak, arXiv:0807.2403 [hep-ph].
- [16] M. Deak, F. Hautmann, H. Jung, K. Kutak, arXiv:1012.6037 [hep-ph];
arXiv:1112.6354 [hep-ph]; arXiv:1112.6386 [hep-ph].
- [17] H. Jung, M. Krämer, A.V. Lipatov, N.P. Zotov, Phys. Rev. D **85**, 034035 (2012);
JHEP **1101**, 085 (2011).
- [18] A.V. Lipatov, G.I. Lykasov, N.P. Zotov, Phys. Rev. D **89**, 014001 (2014);
A.A. Grinyuk, A.V. Lipatov, G.I. Lykasov, N.P. Zotov, Phys. Rev. D **87**, 074017 (2013).
- [19] A. Gawron, J. Kwiecinski, W. Broniowski, Phys. Rev. D **68**, 054001 (2003).
- [20] M.A. Kimber, A.D. Martin, M.G. Ryskin, Phys. Rev. D **63**, 114027 (2001); Eur. Phys. J. C **12**, 655 (2000).
- [21] A.D. Martin, M.G. Ryskin, G. Watt, Phys. Rev. D **70**, 014012 (2004); Eur. Phys. J. C **31**, 73 (2003).
- [22] S. Höche, F. Krauss, T. Teubner, Eur. Phys. J. C **58**, 17 (2008).
- [23] A.D. Martin, M.G. Ryskin, G. Watt, Eur. Phys. J. C **66**, 163 (2010).
- [24] F. Hautmann, M. Hentschinski, H. Jung, arXiv:1205.1759 [hep-ph].
- [25] S. Catani, F. Hautmann, Nucl. Phys. B **427**, 475 (1994); Phys. Lett. B **315**, 157 (1993).
- [26] F. Hautmann, M. Hentschinski, H. Jung, arXiv:1207.6420 [hep-ph].
- [27] H. Jung, G.P. Salam, Eur. Phys. J. C **19**, 351 (2001);
H. Jung et al., Eur. Phys. J. C **70**, 1237 (2010).

- [28] CMS Collaboration, JHEP **1110**, 007 (2011).
- [29] CMS Collaboration, Phys. Rev. D **85**, 032002 (2012).
- [30] CMS Collaboration, Phys. Lett. B **718**, 752 (2013).
- [31] ATLAS Collaboration, Phys. Lett. B **705**, 415 (2011).
- [32] ATLAS Collaboration, Phys. Rev. D **85**, 072004 (2012).
- [33] ATLAS Collaboration, Phys. Lett. B **720**, 32 (2013).
- [34] ATLAS Collaboration, arXiv:1305.4192 [hep-ex].
- [35] LHCb Collaboration, JHEP **1302**, 106 (2013).
- [36] A. Szczurek, G. Slipek, Phys. Rev. D **78**, 114007 (2008).
- [37] A.V. Lipatov, M.A. Malyshev, N.P. Zotov, JHEP **1112**, 117 (2011).
- [38] A. Idilbi, X. Ji, Phys. Rev. D **72**, 054016 (2005).
- [39] J.-P. Lee, Phys. Rev. D **73**, 074012 (2006).
- [40] S. Marzani, R.D. Ball, Nucl. Phys. B **814**, 246 (2009).
- [41] L.N. Lipatov, M.I. Vyazovsky, Nucl. Phys. B **597**, 399 (2001).
- [42] A.V. Bogdan, V.S. Fadin, Nucl. Phys. B **740**, 36 (2006).
- [43] L.N. Lipatov, Nucl. Phys. B **452**, 369 (1995); Phys. Rept. **286**, 131 (1997).
- [44] M. Hentschinski, A. Sabio Vera, Phys. Rev. D **85**, 056006 (2012);
M. Hentschinski, Nucl. Phys. B **859**, 129 (2012);
G. Chachamis, M. Hentschinski, J.D. Madrigal Martinez, A. Sabio Vera, Nucl. Phys. B **861**, 133 (2012).
- [45] J.A.M. Vermaseren, NIKHEF-00-023 (2000).
- [46] H. Jung, arXiv:hep-ph/0411287.
- [47] G. Curci, W. Furmanski, R. Petronzio, Nucl. Phys. B **175**, 27 (1980).
- [48] A.D. Martin, W.J. Stirling, R.S. Thorne, G. Watt, Eur. Phys. J. C **63**, 189 (2009).
- [49] C. Amsler *et al.* (PDG Collaboration), Phys. Lett. B **667**, 1 (2008).
- [50] A. Kulesza, W.J. Stirling, Nucl. Phys. B **555**, 279 (1999).
- [51] G.P. Lepage, J. Comput. Phys. **27**, 192 (1978).
- [52] M. Vesterinen, T.R. Wyatt, Nucl. Instrum. Meth. A **602** 432, (2009).
- [53] A. Banfi, S. Redford, M. Vesterinen, P. Waller, T.R. Wyatt, Eur. Phys. J. C **71**, 1600 (2011).
- [54] V.M. Abazov *et al.* (D0 Collaboration), Phys. Rev. Lett. **106** **106**, 122001 (2011).
- [55] A. Banfi, M. Dasgupta, S. Marzani, Phys. Lett. B **701**, 75 (2011).
- [56] A. Banfi, M. Dasgupta, S. Marzani, L. Tomlinson, JHEP **1201**, 044 (2012).
- [57] A. Banfi, M. Dasgupta, S. Marzani, L. Tomlinson, Phys. Lett. B **715**, 152 (2012).

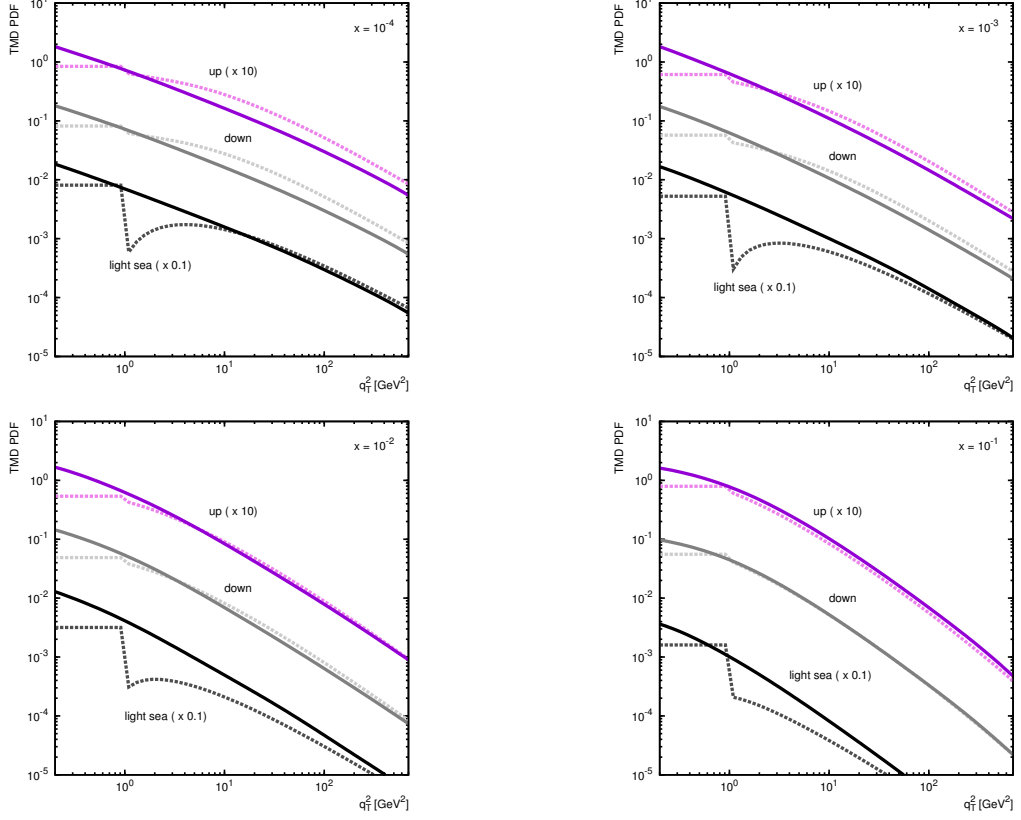


Figure 1: The TMD quark densities $f_q(x, \mathbf{q}_T^2, \mu^2)$ calculated as a function of quark transverse momentum \mathbf{q}_T^2 at several fixed x values and $\mu^2 = m_Z^2$. The solid and dashed curves correspond to the CCFM-based and KMR quark densities, respectively.

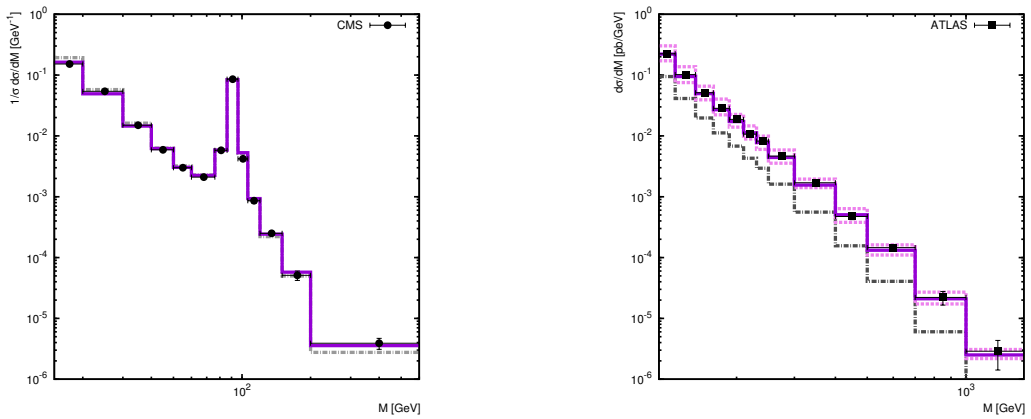


Figure 2: The differential cross sections of Drell-Yan lepton pair production in pp collisions at the LHC as a function of dilepton invariant mass. The solid and dash-dotted histograms correspond to the CCFM-based and KMR predictions, respectively. The upper and lower dashed histograms correspond to the scale variations in the CCFM calculations, as it is described in the text. The experimental data are from CMS [28] and ATLAS [34].

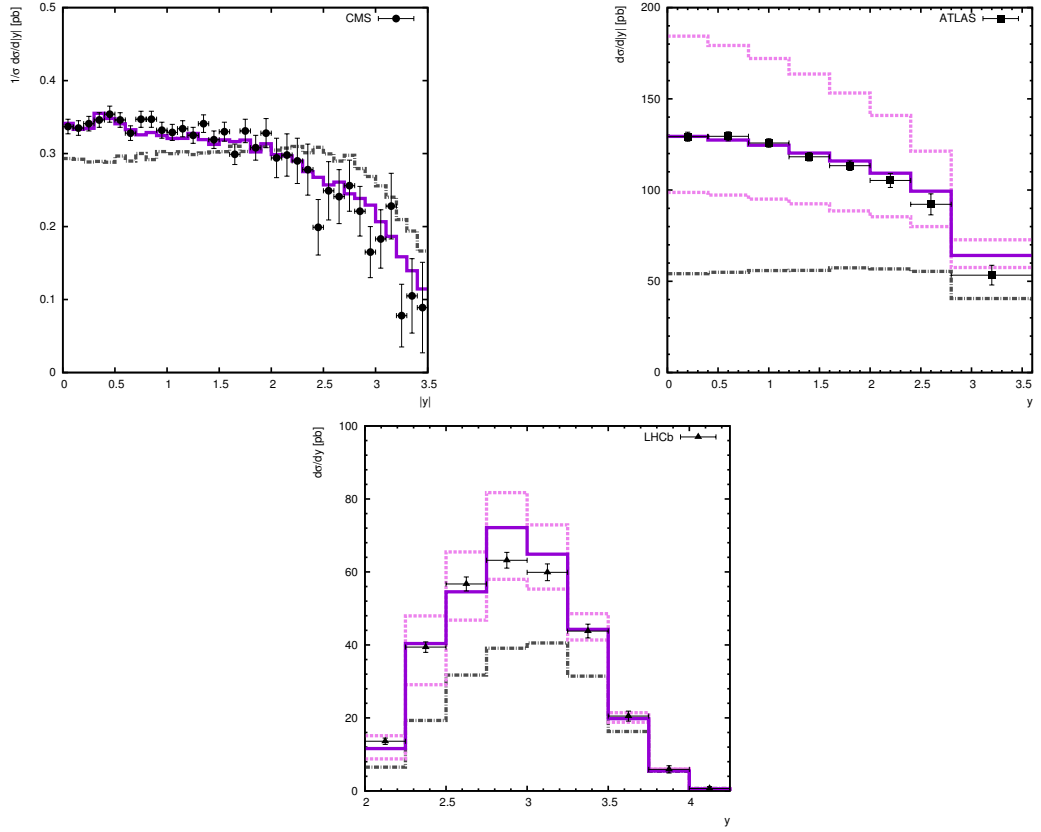


Figure 3: The differential cross sections of Drell-Yan lepton pair production in pp collisions at the LHC as a function of dilepton rapidity y . Notation of all histograms is the same as in Fig. 2. The experimental data are from CMS [29], ATLAS [32] and LHCb [35].

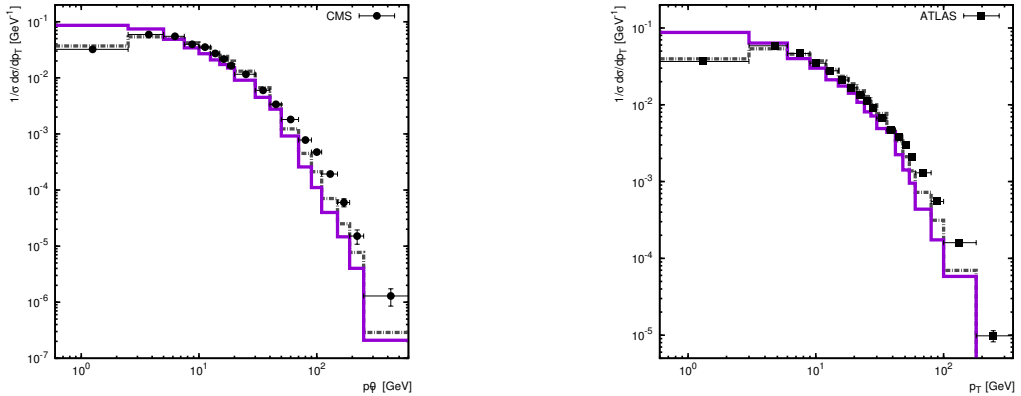


Figure 4: The differential cross sections of Drell-Yan lepton pair production in pp collisions at the LHC as a function of dilepton transverse momentum. Notation of all histograms is the same as in Fig. 2. The experimental data are from CMS [29] and ATLAS [31].

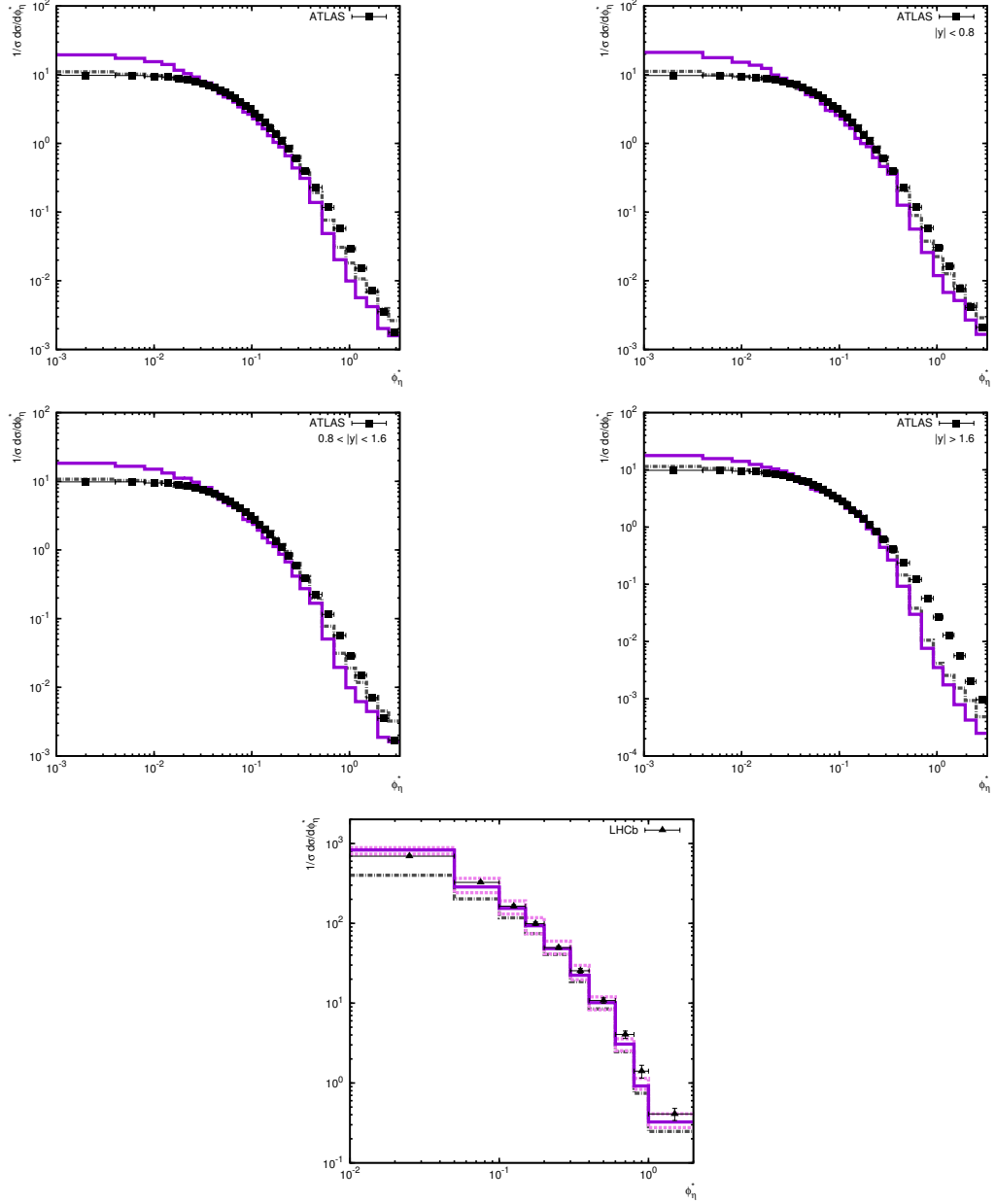


Figure 5: The differential cross sections of Drell-Yan lepton pair production in pp collisions at the LHC as a function of ϕ_η^* . Notation of all histograms is the same as in Fig. 2. The experimental data are from ATLAS [33] and LHCb [35].

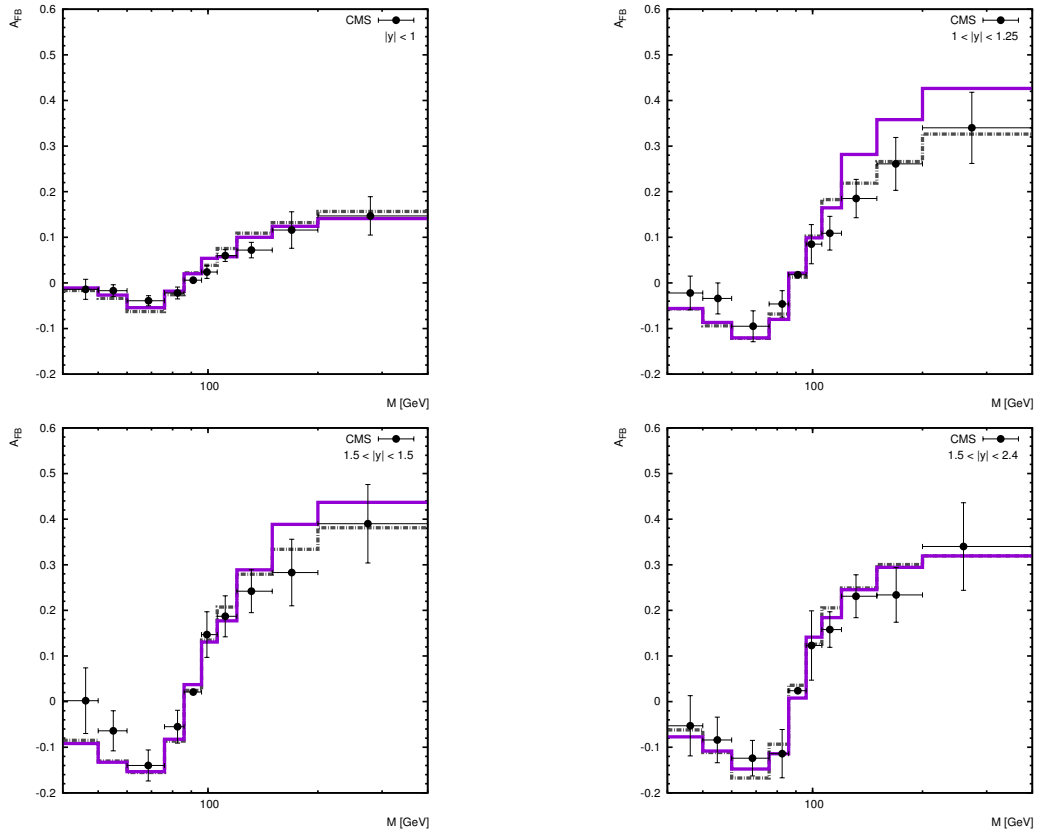


Figure 6: The forward-backward asymmetry A_{FB} calculated as a function of dilepton rapidity and invariant mass. Notation of all histograms is the same as in Fig. 2. The experimental data are from CMS [30].